JOURNAL OF GEOPHYSICAL RESEARCH, VOL. 104, NO. B3, PAGES 4967–4981, MARCH 10, 1999

Evolution of the Australian-Antarctic discordance since Miocene time

Karen M. Marks

Laboratory for Satellite Altimetry, National Oceanic Data Center, NOAA, Silver Spring, Maryland

Joann M. Stock and Katherine J. Quinn[1]

Seismological Laboratory, California Institute of Technology, Pasadena

Abstract. In this study we chronicle the development of the Australian-Antarctic discordance (AAD), the crenelated portion of the Southeast Indian Ridge between ~120° and 128°E, since anomaly 6y time (19 Ma). We reconstruct satellite-derived marine gravity fields and depth anomalies at selected times by first removing anomalies overlying seafloor younger than the selected age, and then rotating the remaining anomalies through improved finite rotations based on a very detailed set of magnetic anomaly identifications. Our gravity field reconstructions reveal that the overall length of the Australian-Antarctic plate boundary within the AAD has been increasing since 19 Ma. Concomitantly, the number of propagating rifts and fracture zones in the vicinity of the discordance has increased dramatically in recent times, effectively dividing it into its present-day configuration of five distinct spreading corridors (B1–B5) that are offset alternately to the north and south and exhibit varying degrees of asymmetric spreading. Our bathymetric reconstructions show that the regional, arcuate-shaped, negative depth anomaly (deeper than predicted by normal lithospheric cooling models) presently centered on the discordance began migrating westward before anomaly 5ad time (~14.4 Ma), and that a localized depth anomaly low, which at time 5ad lay on the ridge axis in spreading corridor B5, has been split apart by subsequent seafloor spreading. The magnetic anomaly patterns suggest that the depth anomaly is not always associated with a particularly contorted plate boundary geometry. Although the plate boundary within the AAD has been getting progressively more crenelated with time, this effect shows little to no migration along the ridge axis since 19 Ma. Thus any geodynamic models of the evolution of the discordance must account for the following observations: (1) the crenelation of the plate boundary within the AAD has increased with time, (2) the center of the crenelated zone does not appear to have migrated along the ridge crest, and (3) both the depth anomaly and the isotopic boundary between Pacific and Indian mantle have been migrating westward along the ridge axis but at apparently different rates. We suggest that both along-axis migration of the depth anomaly and isotopic boundary, as well as temporal variation in the upwelling mantle material beneath the AAD, and local tectonic effects are required in order to explain these observations.

1. Introduction

We have developed a novel approach for examining the evolution of plate boundaries that is particularly well-suited for anomalous or complex regions. Because fine-scale tectonic features of the ocean floor such as fracture zones, transform faults, propagating rifts, and ridge axes are mapped in satellite-derived marine gravity fields [e.g., *McAdoo and Marks*, 1992; *Marks et al.*, 1993], reconstructions of these gravity fields at selected ages in the past can yield details of how plate boundaries evolved over time. A good candidate for this technique is the Australian-Antarctic discordance (AAD), the portion of the Southeast Indian Ridge between about 120° and 128°E, which developed an unusual crenelated ridge pattern in the late Tertiary that has become more exaggerated over time [*Weissel and Hayes*, 1974; *Vogt et al.*, 1983].

The discordance is also anomalous in that a large, arcuate-shaped, negative depth anomaly (deeper than predicted by normal lithospheric cooling models) is centered on it; this depth anomaly trends NNE across the Australian plate (SSE across the Antarctic plate) and is a unique feature on the mid-ocean ridge system. This arcuate pattern suggests a westward migration of the locus of the depth anomaly relative to the Southeast Indian Ridge (SEIR), and conjugate depth anomaly lows on opposite flanks of the spreading ridge suggest that the intensity of the depth anomaly source has varied with time [*Marks et al.*, 1990]. One important aspect of the AAD that we wish to examine is the relationship between the depth anomaly and the crenelated geometry of the plate boundary; that is, are they spatially correlated, and do they vary similarly in intensity with time? Has the very crenelated section of the plate boundary been migrating westward along with the depth

[1]Now at Department of Earth and Planetary Sciences, Massachusetts Institute of Technology, Cambridge.

Paper number 1998JB900075.
0148/0227/99/1998JB900075$09.00

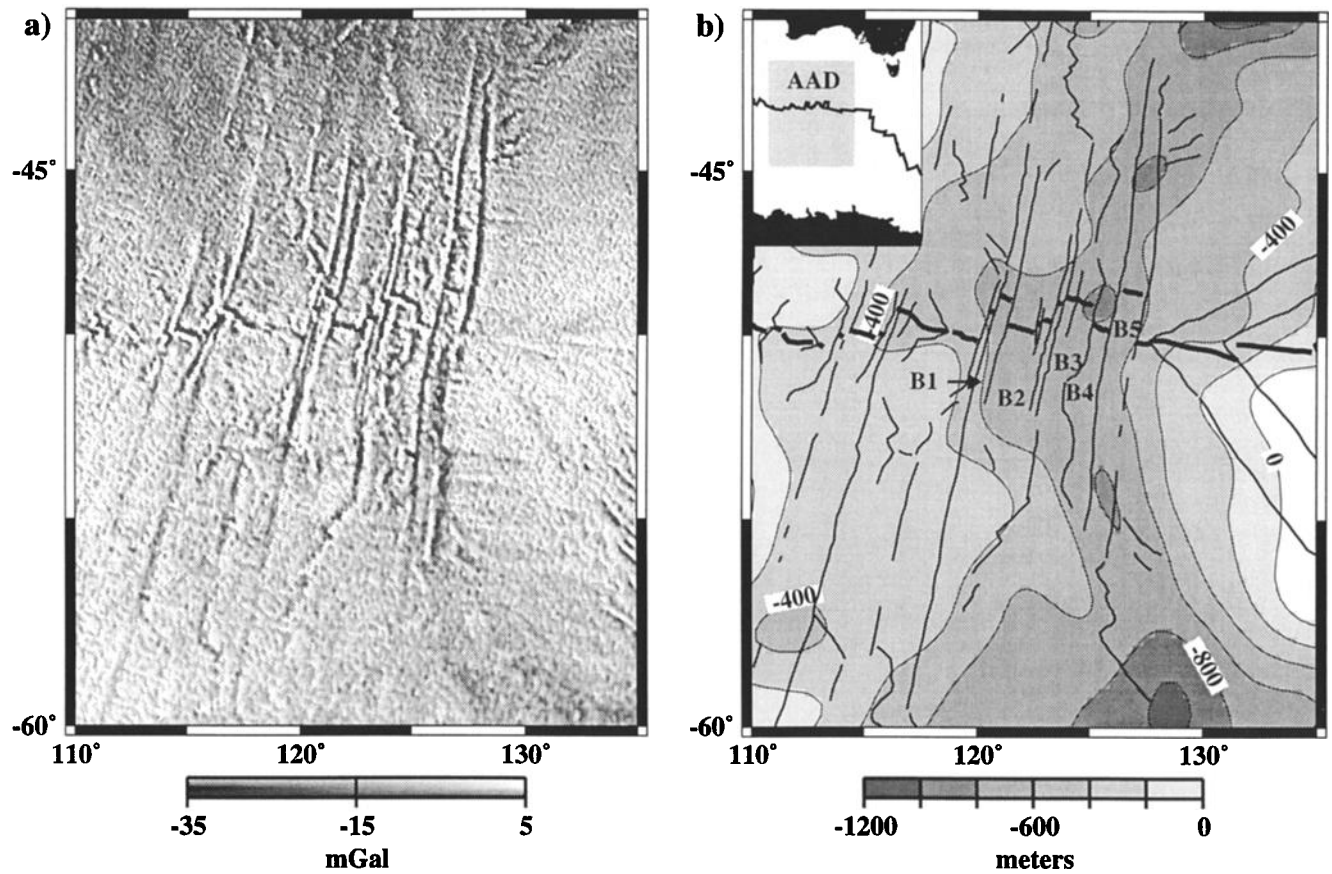

Figure 1. (a) Shaded relief image of satellite-derived gravity anomalies covering the Australian-Antarctic discordance. Gravity anomalies range between ≤ -35 mGal and ≥ 5 mGal and are "illuminated" from the northeast. (b) Depth anomalies over the discordance. Thin lines are depth anomaly contours (200 m contour interval), medium lines are fracture zones and propagating rifts, and heavy lines are ridge segments. Spreading corridors B1–B5 are notated following *Vogt et al.* [1983].

anomaly? If so, both the depth anomaly and the crenelated plate boundary geometry might represent manifestations of the same mantle process. Our reconstructions reveal when the migration and intensity variations of the depth anomaly took place and demonstrate their relationship to the increasingly complex ridge segmentation pattern that is chronicled in the reconstructed gravity fields and the geometry of the magnetic isochrons.

2. Data

We used the portion of the marine gravity field of *Sandwell and Smith* [1997] covering the discordance (Figure 1a) as the basis of our gravity reconstructions. As pointed out in section 1, satellite-derived gravity anomalies such as these map tectonic details of the seafloor. For example, in Figure 1a, the Southeast Indian Ridge trends east-west along about −50° latitude; west of the bounding transform at ~128°E are prominent axial valleys (negative gravity anomalies), while to the east is an axial high (positive gravity anomalies). The ridge segments are offset alternately to the north and south by transform faults, and fracture zones appear as long, linear gravity anomaly lows trending perpendicular to the spreading ridge. In order to retain the highest resolution in our reconstructed gravity fields we resampled the Sandwell and Smith grid (which is provided in Mercator projection) onto a regular 2 min (longitude) by 1.5 min (latitude) grid.

To determine finite rotations and to form our seafloor age grid, which is needed to compute predicted depths, we used a new, very detailed set of picks of seafloor magnetic anomalies, based on aeromagnetic data from the Project Investigator survey [*Morgan et al.*, 1979], and available ship magnetic data [*National Geophysical Data Center*, 1997]. We deskewed the aeromagnetic profiles shown in Figure 2 and along with the available ship track data identified more than 4630 magnetic anomaly points in the discordance zone and adjacent regions (Figure 3). Ages were assigned to the magnetic anomalies and isochrons according to the reversal chronology of *Cande and Kent* [1995]. Note that many of our picks lie within the discordance region, where detailed magnetic anomaly picks are often omitted in other studies [e.g., *Royer and Gordon*, 1997]. The details of the magnetic anomaly picks within the AAD itself are not critical to determination of the overall past relative positions of the Australia and Antarctica plates; however, they do provide key constraints on the evolution of the ridge crest geometry in the discordance through time and hence were of particular interest in our study. Owing to the extent of the aeromagnetic coverage, the oldest magnetic anomaly identified with this level of detail was 7 on the northern ridge flank and 6o to the south; within the AAD itself the oldest magnetic

anomaly well-covered on the southern side is 6y (Figure 3). We thus limit our calculation of the finite rotations, and our discussion of the detailed ridge geometry and the gravity field reconstructions, to times 6y and younger.

The finite rotations for the past relative positions of Australia and Antarctica in this region were determined using the detailed magnetic anomaly identifications with constraints from fracture zones that are accurately located in the marine gravity fields [*Marks and Stock*, 1991] (Table 1). For nearly all of the rotations, we used data between about 115° and 137°E. However, for chron 6y we incorporated data from 99°E to 137°E, including ship tracks and fracture zone picks from Geosat data outside the detailed study area. We used the technique of *Hellinger* [1981] to do a grid search for the best fit rotation (pole and angle) to match data points from the two sides, using software developed by *Chang* [1987, 1988]. The data points were divided into counterpart segments (magnetic anomaly segments or fracture zone segments) from each plate, with errors assigned according to the type of location uncertainty inherent in the data and the along-track uncertainty in picking the position of the magnetic reversal or fracture zone. Uncertainties in the resulting finite rotations are described by covariance matrices (Table 2) according to the technique of *Chang* [1987, 1988], which is also discussed by *Royer and Chang* [1991]. The covariance matrix is given by

$$\frac{1}{\hat{\kappa}} * \begin{pmatrix} a & b & c \\ b & d & e \\ c & e & f \end{pmatrix} \times 10^{-g}$$

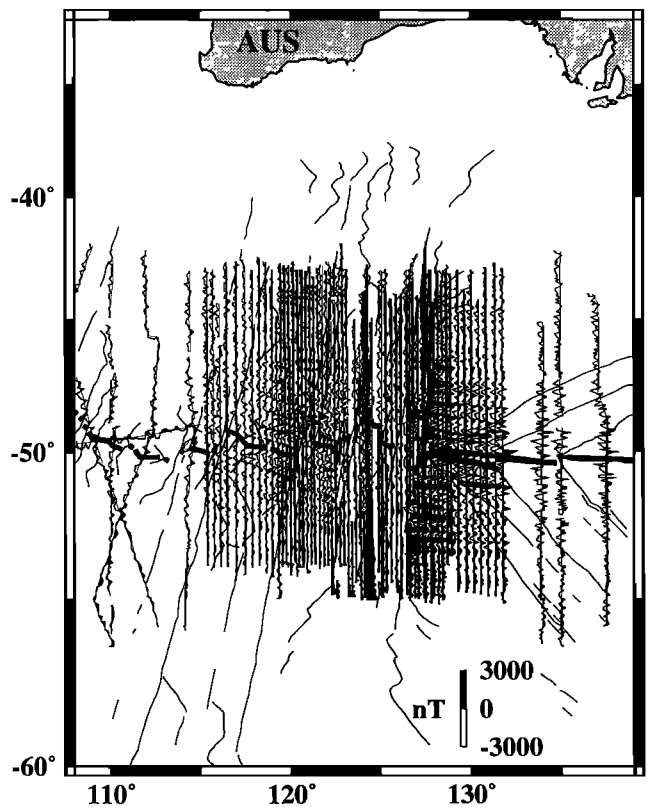

Figure 2. Project Investigator residual magnetic anomaly profiles plotted along flight tracks [*Morgan et al.*, 1979] and ship tracks *Eltanin* 34, 39, 41, 45, 47, 49; *Glomar Challenger* 28; and *Melville* 5.

Table 1. Finite Rotations of Australia Relative to a Fixed Antarctic Plate

Magnetic Anomaly	Age, Ma	Latitude, °S	Longitude, °W	Angle, deg
6y	19.048	13.449	145.339	11.48
5ad	14.395	11.2129	142.7252	8.77
5o	10.949	11.4937	141.5066	6.81
4	7.752	14.5478	141.6163	5.02
3ay*	5.894	12.6122	139.2836	3.84
3y	4.235	14.4472	140.5404	2.73
2ay	2.581	16.2062	141.3136	1.67

Counterclockwise rotations are positive. Ages are from *Cande and Kent* [1995].

*A chron for which a finite rotation was determined but which was so close in time to subsequent and preceding chrons that we do not show the corresponding reconstructions.

where the values a–f are given in radians squared. Note that the covariance matrix depends on the uncertainties assigned to the data, and may be rescaled by a value $\hat{\kappa}$ which indicates whether the uncertainties assigned to the data are overestimated or underestimated [see *Royer and Chang*, 1991]. Note that because the rotations for 5ad and younger times are based on a very limited east-west length of the entire Australia-Antarctica plate boundary, they have larger errors than would be expected if data from the entire length of the plate boundary were used.

For the region beyond the aeromagnetic survey we used the magnetic anomaly isochrons from *Müller et al.* [1997] to define the seafloor age grid. We then computed the mean age and position (i.e., the mean latitude and longitude) within each 0.25° grid cell that contained data, and finally, we gridded these mean values onto a regular 0.25° latitude and longitude grid.

We chose the thermal boundary layer model [*Turcotte and Oxburgh*, 1969] to predict the relationship between the depth of the seafloor and its age:

$$\text{depth} = d_0 + C(\text{age}^{1/2})$$

where d_0 is the ridge crest depth, C is the subsidence constant, and age is from the grid we described above. We chose the d_0 value of 2700 m and the subsidence constant of 350 m/m.y.$^{1/2}$, which *Cochran* [1986] determined best fit the ridge crest depth and normally subsiding ridge flanks east and west of the discordance (with exception of the northern flank east of the AAD, which is subsiding at an unusually high rate). Increasing the constant d_0 (e.g., to 2900 or 3000 m) would increase the negative depth anomaly amplitudes by 200 or 300 m without changing their shape, while reducing the subsidence constant C (e.g., to 300 m/m.y.$^{1/2}$) would make the depth anomalies more negative (i.e., larger amplitude) on the flanks relative to the ridge crest (e.g., ~225 m at 20 Ma).

To calculate the depth anomalies shown in Figure 1b, we subtracted these predicted depths from the bathymetric grid published by *Smith and Sandwell* [1994], after first correcting the bathymetry data for sediment loading (D. Divins, sediment thickness data, report in preparation, 1998). Although the bathymetric depths in the Smith and Sandwell grid are actually estimated from a combination of satellite-derived gravity anomalies (for wavelengths <160 km) and ship soundings (for wavelengths >160 km), they demonstrated that their grid, in fact, does a better job mapping the seafloor than the ETOP05 grid [*National Geophysical Data Center*, 1988], which was com-

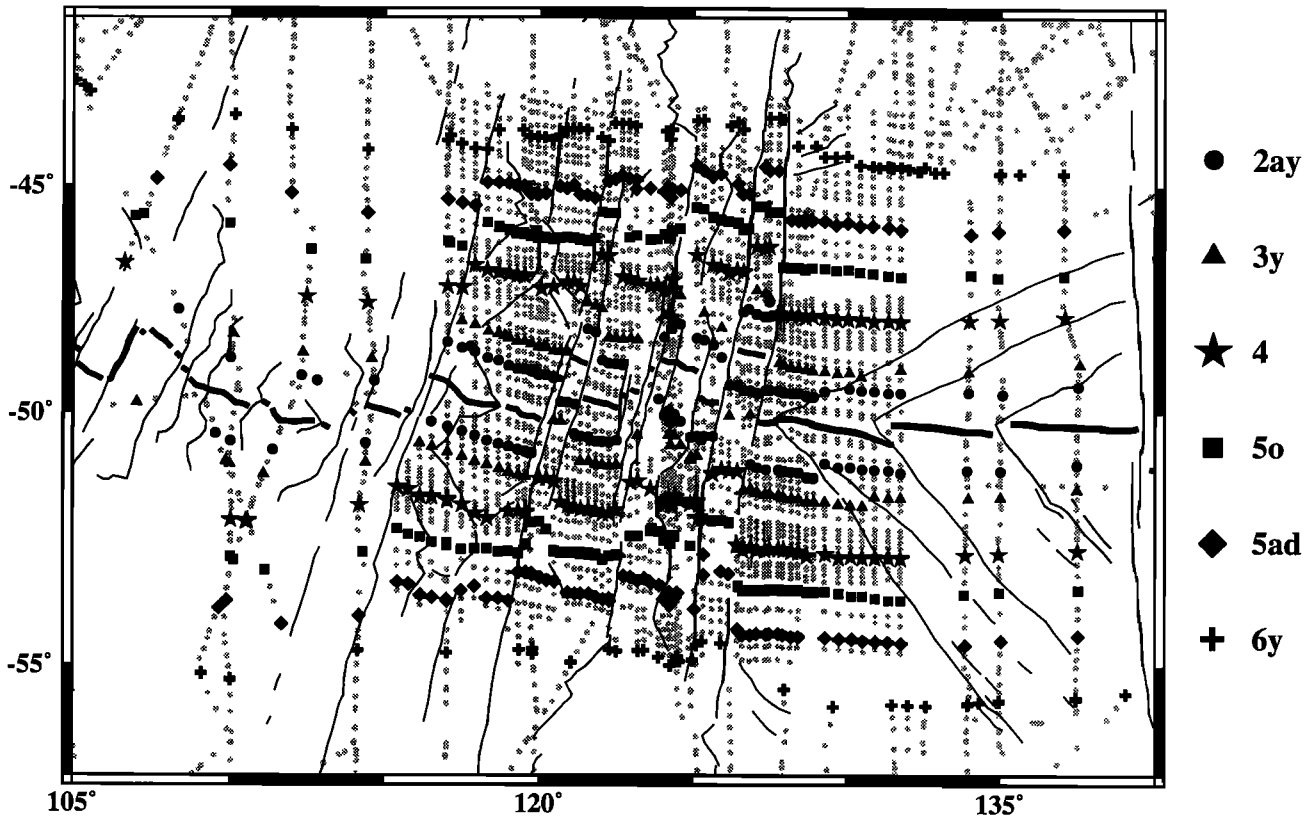

Figure 3. Magnetic anomaly identifications from the aeromagnetic survey [*Morgan et al.*, 1979] and available ship track data. Shaded circles are magnetic anomaly identifications, and solid symbols (notated in figure) are identifications relevant to our selected reconstruction times.

piled solely from ship observations [see *Smith and Sandwell*, 1994, Figure 8]. Because we are using the estimated depths solely to obtain a depth anomaly solution suitable for our reconstructions and the *Sandwell and Smith* [1997] field solely for gravity reconstructions, it does not matter that the gravity and depth anomaly grids are, in fact, dependent, as it would if they were used together in an admittance calculation, for example.

The depth anomalies were then high-cut filtered with a cosine tapering function to pass anomalies with wavelengths greater than 400 km. Following *Menard* [1973], we define an area deeper than predicted as having a negative depth anomaly. The resulting depth anomalies shown in Figure 1b are in excellent agreement with previously published maps [e.g., *Hayes*, 1988; *Marks et al.*, 1990] and provide anomalies in the digital form needed for our reconstruction method. This excellent agreement between depth anomalies computed using *Smith and Sandwell*'s [1994] estimated depths compared to depth anomalies based on topography-only solutions reflects how well Smith and Sandwell's predictions match longer wavelength topography, particularly at wavelengths >400 km as remain in our depth anomaly grid after high-cut filtering and resampling onto a 0.25° grid.

3. Method

To form the gravity and depth anomaly reconstructions shown in Figures 4a–4f, we first removed corresponding anomalies overlying seafloor younger than the selected time. Where available, we used magnetic anomalies identified in the detailed magnetic survey and ship data (Figure 3) or published anomaly isochrons [*Müller et al.*, 1997] to define the seafloor isochrons. Where magnetic data were lacking, we estimated the isochrons using available older and/or younger isochrons as

Table 2. Covariance Matrices for Finite Rotations Given in Table 1

Anomaly	Age, Ma	$\hat{\kappa}$	a	b	c	d	e	f	g
6y	19.048	1.25	3.11	−3.91	4.39	7.11	−7.21	9.11	7
5ad	14.395	0.074	5.16	−6.83	6.42	9.51	−10.44	23.56	8
5o	10.949	0.059	5.58	−7.11	5.74	9.46	−9.11	20.62	8
4	7.752	0.065	7.43	−9.36	8.60	12.28	−12.38	19.86	8
3ay	5.894	0.043	5.65	−6.72	3.86	8.34	−5.90	10.6	8
3y	4.235	0.098	3.58	4.20	2.34	5.31	−4.25	8.80	8
2ay	2.581	0.14	4.08	−4.82	3.55	6.08	−5.62	9.89	8

Ages are from *Cande and Kent* [1995].

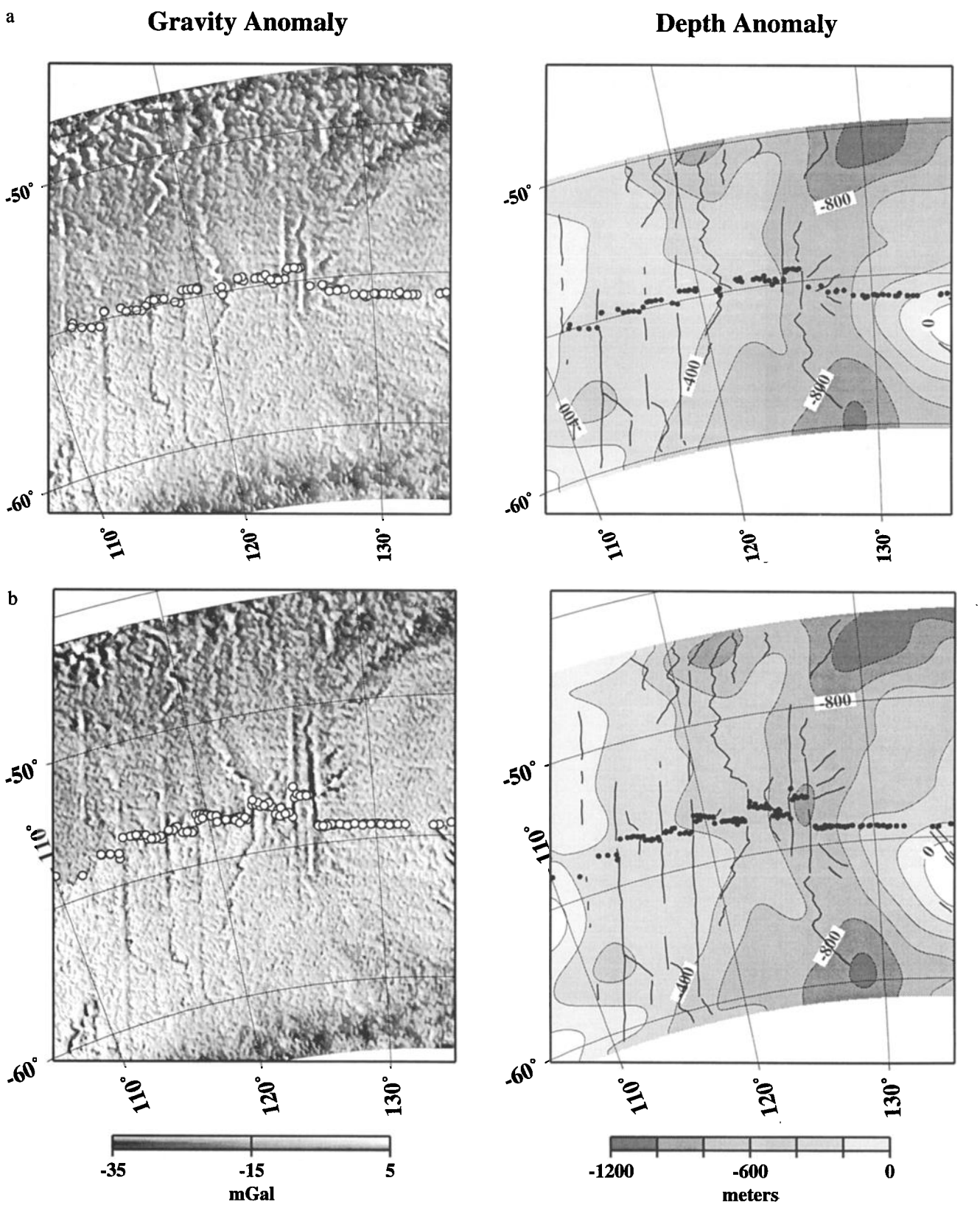

Figure 4. Gravity field and depth anomaly reconstructions for Chrons (a) 6y, (b) 5ad, (c) 5o, (d) 4, (e) 3y, and (f) 2ay. The Antarctic plate is held fixed. The shaded relief gravity images are "illuminated" from the east, and depth anomalies are contoured as in Figure 1b. Magnetic anomalies 6y, 5ad, 5o, 4, 3y, and 2ay, identified from aeromagnetic and ship data, are white circles on corresponding gravity (solid circles on depth) anomaly maps. These images are plotted using an oblique Mercator projection, substituting the finite rotation pole as the projection pole.

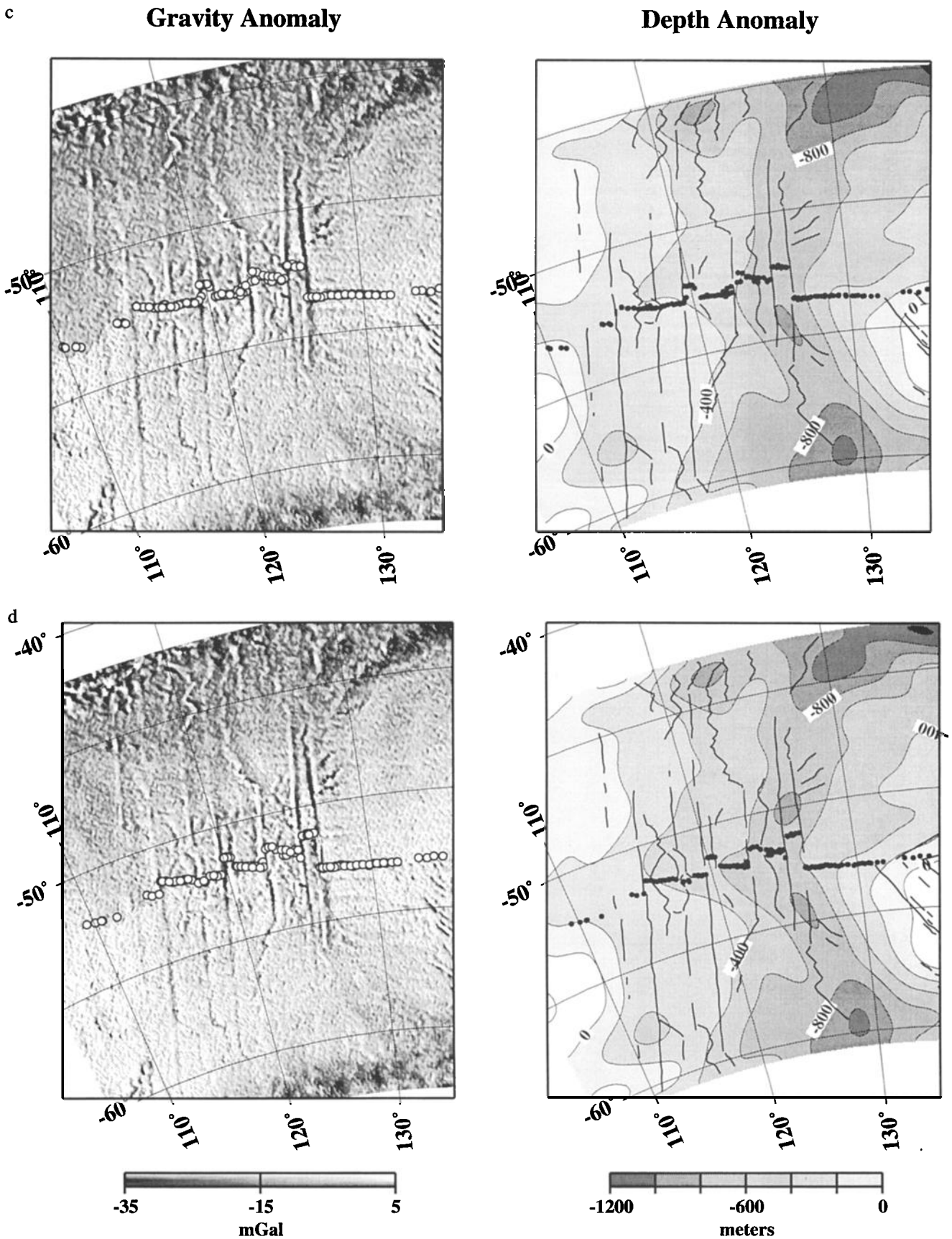

Figure 4. (continued)

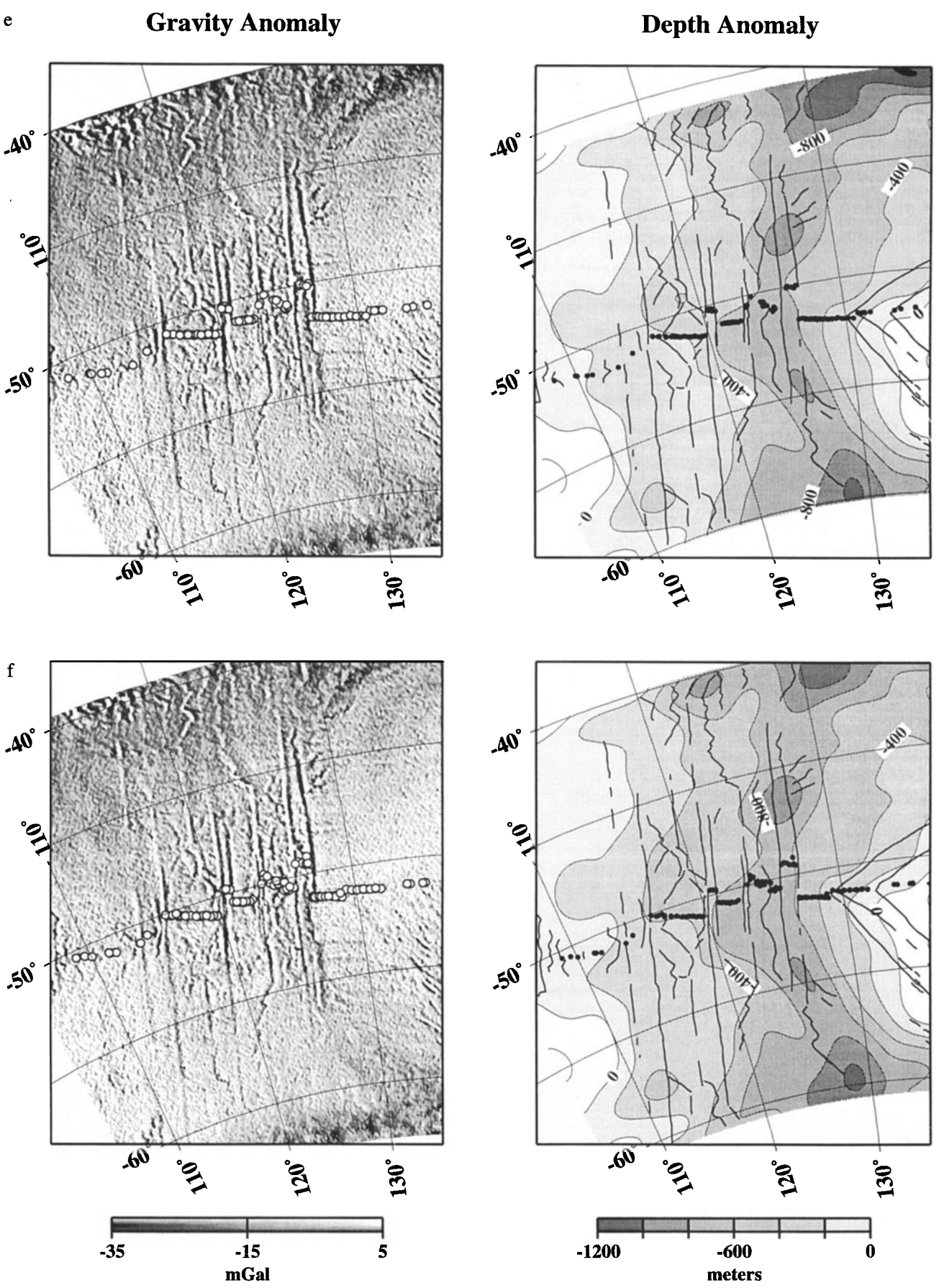

Figure 4. (continued)

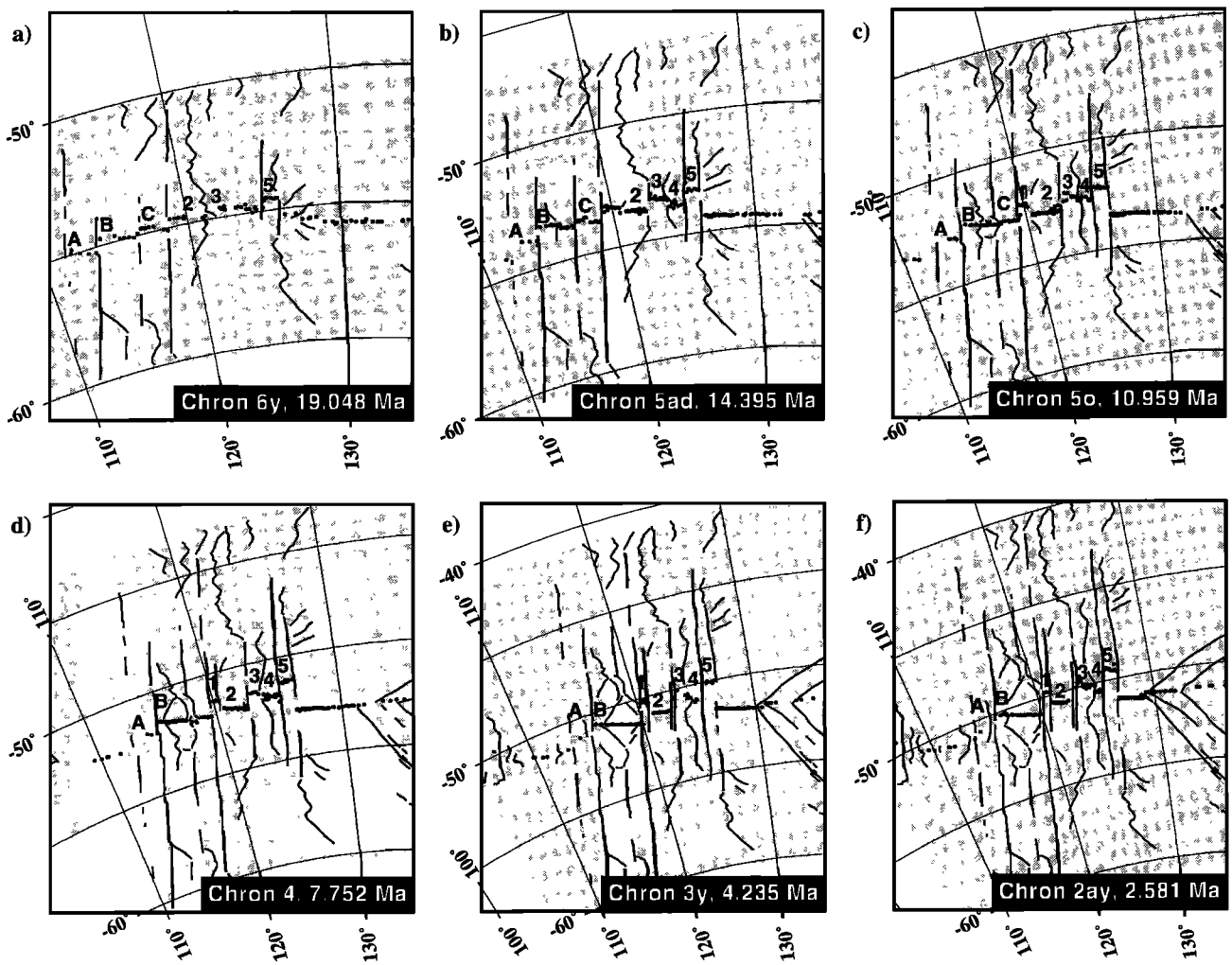

Figure 5. Tectonic sketches of the evolving discordance zone at selected times. Medium lines are fracture zones and propagating rifts; circles are corresponding magnetic anomaly identifications. The projection is described in the Figure 4 caption.

a guide, and in their absence, we rotated the ridge axis that is mapped in the gravity anomalies outward by the appropriate finite rotation. Combining these observed and predicted seafloor ages provided isochrons delineating the younger anomalies to be removed. To complete the reconstructions, we "rolled back" spreading on the Southeast Indian Ridge, effectively moving the remaining (older) Australian gravity and depth anomalies towards a "fixed" Antarctic plate by using the appropriate finite rotations (Table 1). The resulting reconstructions successfully align, across the paleospreading ridge, conjugate fracture zone traces that are embedded in the Australian and Antarctic plates. This confirms that our improved finite rotations are very accurate.

4. Results

4.1. Plate Boundary Changes Through Time

For reasons pointed out earlier, the tectonic development of the discordance is best viewed in the gravity reconstructions. We note here that because the large fracture zones trend N10°E through the study area (see Figure 1a), as seafloor has been accreted to the Antarctic plate and the SEIR migrated northward, the intersections between the fracture zones and the spreading ridge have moved eastward over time relative to the established latitude and longitude grid attached to the fixed Antarctica plate. Thus for simplicity, in this section, we refer to the tectonic sketches in Figures 5a–5f to denote the features discussed rather than list their locations at each age chron.

Our reconstructions show that the overall length of the plate boundary within the AAD has increased since Chron 6y (Table 3). For the time of each reconstruction we digitized 50–100 points along the plate boundary between the eastern end of the spreading segment just west of the AAD and the eastern transform fault bounding segment B5 of the AAD (thick lines in Figure 6). We then calculated the length of the active plate boundary (transform faults and ridge segments) represented by the digitized points (Table 3 and Figure 7). These measurements demonstrate that between Chron 6y (19 Ma) and Chron 2ay (2.6 Ma) the plate boundary in this sector became progressively more crenelated with time. We find no major difference in length of the plate boundary between Chron 2ay and the present. The progressive increase in crenelation appears to be confined to the region of the AAD itself; the active plate boundary between fracture zone B (west of the AAD, Figure

Table 3. Length of Australia/Antarctica Plate Boundary Through Time Within the AAD

Anomaly	Age, Ma	Length, km
6y	19.048	662
5ad	14.395	814
5o	10.949	838
4	7.752	919
3y	4.235	1030
2ay	2.581	1083
0	0	1093

Ages are from *Cande and Kent* [1995].

6) and the western limit of the AAD does not show any similar increase in length through time. Our calculations are somewhat dependent on the data coverage available. However, the detailed magnetic anomaly coverage provided by the aeromagnetic survey allows us to be confident that our comparison of plate boundary length through time is valid. Present coverage of the magnetic anomalies by ship tracks beyond the detailed study area is too sparse to allow us to extend these calculations to the entire length of the Australia-Antarctica plate boundary, or to older times.

The detailed kinematics of how the plate boundary has lengthened through time in this sector can be appreciated by a comparison of successive frames of the gravity grid reconstructions. Our oldest reconstruction is that for Chron 6y (19 Ma), which is shown in Figure 4a. At this time, the discordance consisted of only a central, eastward pointing pseudofault pair between spreading corridors B2 and B3 (Figure 5a) and three large fracture zones, two of which have persistently bracketed ridge segment B5 and the third of which bounds the AAD on the west. To the west of the discordance are three major fracture zones (A, B, and C in Figure 5a). These fracture zones and others were originally very sinuous adjacent to the continental margins, where they are embedded in seafloor formed during the initial (older than 43 Ma), slow separation of Aus-

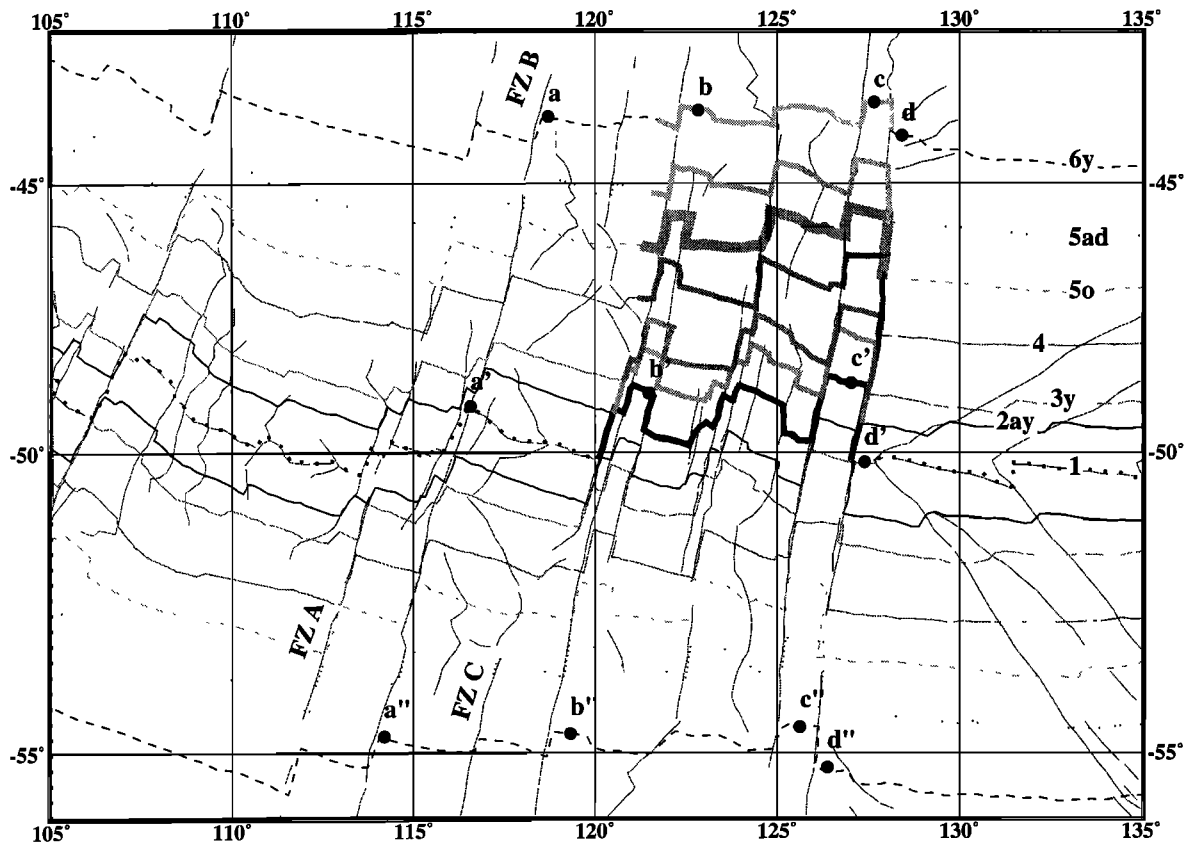

Figure 6. Isochrons delineating paleoplate boundary length. For the present time the length is measured from the eastern end of the spreading segment just west of the discordance (50.125°S, 120.08°E) to the western end of the spreading segment just east of the discordance (50.125°S, 126.991°E) (thick solid line). For past times the plate boundary is reconstructed using the detailed magnetic anomaly picks (Figure 3) and finite rotations (Table 1), and its length is measured between the equivalent two points tracked back along the plate separation direction (shown by thick shaded lines), parallel to the fracture zone at 127°E. For each time period, ~50–100 points were defined evenly spaced along the plate boundary and were used to calculate the length. Points a′, b′, c′, and d′ along the present plate boundary were used to evaluate the degree of asymmetric spreading in various segments of the ridge system. Their conjugate points a–d lie on the 6y isochron on the Australia plate; their conjugate points a″–d″ are on the 6y isochron on the Antarctica plate. The distance a–a′ and a′–a″ are about the same (5.7°, 5.8°), suggesting that the spreading in the segment just east of fracture zone (FZ) B has been symmetric since Chron 6y. By contrast, distances b–b′ (5.5°) and c–c′ (5.4°) on the Australia plate are consistently shorter than the counterpart distances on the Antarctica plate (5.9°). Distance d–d′ is 6.1°, longer than the counterpart distance d′–d″ of 5.1° on the Antarctica side.

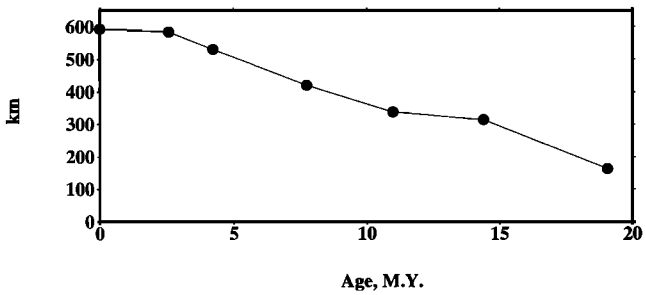

Figure 7. Graph of the excess length of the plate boundary within the AAD as a function of time since Chron 6y (19 Ma). Excess length is relative to the length of an uncrenelated ridge axis (which we estimate to be ~500 km).

tralia from Antarctica [*Cande and Mutter*, 1982]. East of the discordance are the tips of two westward propagating spreading segments with associated pseudofault traces opening to the east; the outermost has already terminated against the fracture zone bounding the AAD on the east, and the innermost is approaching it. Also east of the AAD is a regional, arcuate-shaped gravity anomaly low of unknown origin that trends NNE on the Australian plate (SSE on the Antarctic plate).

By Chron 5ad (14.4 Ma), the spreading segment between corridors B2 and B3 had ceased its eastward propagation so that its eastern boundary, which had been a pseudofault or a wandering offset, became a fracture zone. Small, unstable offsets developed between the nascent spreading corridors B1 and B2 and B3 and B4 and between fracture zones B and C west of the AAD (Figures 4b and 5b). The offsets between corridors B1 and B2 and B3 and B4 changed migration direction and began migrating westward by Chron 5o time (11 Ma), while fracture zone C west of the discordance (Figures 4c and 5c) turned into an eastward pointing pseudofault pair or wandering offset due to eastward propagation of the spreading segment on its west side.

By Chron 4 time (7.8 Ma), dueling spreading centers formed between fracture zone B and the former fracture zone C west of the discordance (Figures 4d and 5d). At the same time, the boundary between corridors B1 and B2 stabilized and turned into a fracture zone, whereas the boundary between corridors B3 and B4 continued its westward migration. The pseudofault pattern becomes even more complicated by Chron 3y time (4.2 Ma) because not only did several pseudofaults terminate against fracture zone B and the fracture zone that bounds the discordance on the west (Figures 4e and 5e), but a new pair of pseudofaults formed in their wake. In addition, the boundary between corridors B3 and B4 was a transform fault between anomaly 4 and 3y times, but by 3y, it had changed into an eastward pointing pseudofault. Also, at Chron 3y time the fracture zone between corridors B2 and B3 is flanked by a smaller fracture zone.

Our youngest reconstruction, for Chron 2ay (2.6 Ma), is shown in Figures 4f and 5f. By this recent time, an additional small fracture zone flanks the fracture zone bounding the AAD on the west, and the boundary between corridors B3 and B4 continues its eastward migration. Further, additional small, unstable eastward pointing pseudofaults have formed west of the AAD. We note that the regional, arcuate-shaped gravity anomaly low that we pointed out earlier does not have a clear expression within the discordance in these younger reconstructions. We cannot determine from these gravity images if the regional gravity low exists within the AAD but is masked by the more prominent short-wavelength gravity anomalies arising from the complicated tectonics.

To summarize, in the span of 20 m.y., the discordance developed from a spreading ridge that was crossed by a few major fracture zones to a ridge characterized by numerous fracture zones and pseudofault pairs that offset the ridge segments in an unusual crenelated pattern. The most distinctive development revealed by our gravity reconstructions is that many of the fracture zones in the discordance formed initially from unstable or wandering offsets (pseudofault pairs). The exception is the unusual boundary between spreading corridors B3 and B4 which has, at different times, been either a westward pointing pseudofault, an eastward pointing pseudofault, or a stable transform fault. These transitions between boundary types have caused the adjacent ridge segments to lengthen and shorten over time.

Small ridge jumps have been confirmed in the discordance [e.g., *Vogt et al.*, 1983; *Marks and Stock*, 1995], and in spreading corridor B4 the recent southward jump of the ridge axis occurred at a time when the ridge segment was short in length. There is an east-west trending gravity low north of the anomaly 5ad identifications in corridor B3 (see Figure 4b) that appears to be the scar of an older ridge jump. This jump also took place when the ridge segment (B3) was short in length. A similar scenario is recorded west of the discordance; there is an east-west trending gravity low that extends west of fracture zone C to the unstable propagating rift in that spreading corridor (see Figure 4c, west of fracture zone C and south of the 5o anomaly identifications) that is consistent with the signature of a ridge jump that occurred when the ridge segment length was short. This suggests that there may be a relationship between the length of a ridge segment and ridge jumps; possibly, a shorter ridge segment jumps more easily.

Along spreading-transform boundaries, changes in the direction of relative plate motion can produce lengthening or shortening of the plate boundary as the new direction of spreading is accommodated by modifications in transform fault geometry and ridge segmentation, including the development of nontransform offsets [e.g., *Tucholke and Schouten*, 1989; *Lonsdale*, 1995]. This is normally accomplished by systematic increases in offset along fracture zones or ridge offsets of one polarity and decreasing offsets along fracture zones of the opposite polarity (e.g., the overall length of the plate boundary in regions of right-stepping fracture zones increases, whereas in regions of left-stepping fracture zones it decreases). However, there is no such simple relationship between the relative plate motions and the changes in plate boundary geometry within the AAD. The finite reconstruction poles for anomalies 2ay, 3y, 3ay, 4, and 5o have overlapping uncertainty regions at the 95% confidence level (Figure 8). This is partly because of the short length of plate boundary used to determine these finite rotations; addition of more detailed picks of these anomalies farther from the AAD would help these uncertainty regions to shrink further. We can resolve a change in the finite rotation pole between Chron 4 and Chron 5ad, and again between Chron 5ad and Chron 6y, but the resultant effect on transform fault orientations would be expected to be minor. More importantly, during the lengthening of the plate boundary within the discordance, offsets on both left-stepping and right-stepping transform faults have increased (i.e., spreading segments B1, B3, and B5 have migrated northward relative to adjacent spreading segments; see Figures 5a–5f). This suggests

that a simple change in the direction of relative plate motion cannot explain the progressive lengthening of the plate boundary.

It has been noted that along many spreading centers, the planform of spreading-transform systems depends on the overall magma budget compared to the amount of "tectonic tension" in a given region, with higher magma supplies leading to simpler geometries with more continuous ridge segments and fewer transform or nontransform offsets [*Abelson and Agnon*, 1997]. However, the cases examined by *Abelson and Agnon* [1997] all were interpreted with systematic, en echelon offsets of the spreading centers, unlike the geometry of major right-stepping and left-stepping offsets in close proximity, which is characteristic of the discordance. Thus a more complicated model and/or a different process seems needed to explain the development through time of the plate boundary in the region of the AAD.

We examined the degree of asymmetry present in several of the spreading segments in order to quantify the development of the crenelated geometry of the plate boundary. For example, since Chron 6y, the segment immediately to the east of fracture zone B (117°E on the ridge crest) has been spreading symmetrically; the distance between point a, on the Australia 6y isochron, and point a′, on the ridge crest, is the same as between the ridge crest and the conjugate point (a″) on the Antarctica 6y isochron (see Figure 6). Segments 1 and 5 within the discordance (points b and c, Figure 6) have been spreading asymmetrically, with more crust accreted to the Antarctica side in both cases than to the Australia side. Interestingly enough, the ridge segment just east of the discordance exhibits the opposite behavior, with more crust accreted to the Australia side than to the Antarctica side (point d, Figure 6) [*Vogt et al.*, 1983].

An additional important point regarding the evolution of the plate boundary within the AAD is that the pattern of crenelation shows little to no migration parallel to the ridge axis since 19 Ma. For example, if the crenelation were caused by a point source moving from east to west, one might expect that the eastern end of the discordance developed more crenelation early on and that increases in crenelation on the western side of the discordance would have occurred at younger times. However, the increases in crenelation appear to be fairly evenly distributed along the plate boundary at all times. As mentioned above, segments B1, B3, and B5 have migrated north faster than the adjacent spreading segments; in these cases, migration was occurring as far back in time as we have resolution (between Chrons 6y and 5ad). One could argue there is a hint of slight westward migration of the crenelation pattern from two observations. First, the youngest changes in the plate boundary geometry seem to be more pronounced in segment B1 than in segment B5; second, there were some pseudofaults disrupting the western end of the spreading segment just east of the AAD at Chron 6y (Figure 4a), and this ridge segment subsequently straightened out, reducing its overall length slightly. Detailed magnetic anomaly observations for older seafloor in the region would be necessary to thoroughly evaluate the possibility of progressive westward migration of the crenelated plate boundary zone for older times. However, in general, for the time period we are studying (post-19 Ma), the crenelation does not seem to have moved laterally along the ridge axis.

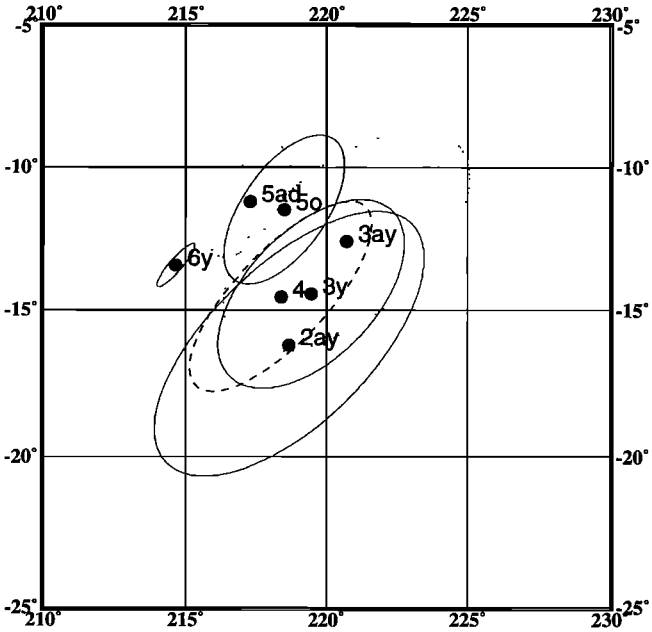

Figure 8. Map of the best fit pole positions for reconstructing the past position of Australia relative to Antarctica (Table 1) and the 95% confidence limits for the pole locations, derived from the covariance matrices for the rotations (Table 2). For clarity, the uncertainty region for the Chron 4 pole is dashed; those for Chrons 5ad and 3ay are dotted. Note that the uncertainty regions for Chrons 2ay, 3y, 3ay, and 4 all overlap. The uncertainty region for the Chron 6y pole is small compared to the others because a longer section of the plate boundary was used and the rotation is better determined (note that the value of $\hat{\kappa}$ in Table 2 is close to 1).

4.2. Evolution of the Depth Anomaly Through Time

Now that the tectonic development of the discordance has been detailed using the gravity reconstructions, we turn to the depth anomaly reconstructions. We reiterate here that our reconstructions "roll back" seafloor that has been generated on the SEIR; thus we effectively "roll back" the depth anomaly too because we make the simple assumption that it is embedded in the seafloor. If the depth anomaly is purely dynamically maintained, then our reconstructions have no bearing on the past history of the depth anomaly; however, the presence of thinner than normal oceanic crust along the AAD [*Tolstoy et al.*, 1995] suggests that part of the depth anomaly is due to isostasy and would therefore be embedded in the seafloor in the sense that it would correspond to locations of thinner crust. (Future off-axis refraction measurements are needed to independently measure the crustal thickness throughout the area of the present depth anomaly.) *Gurnis et al.* [1998] suggest that about half of the present depth anomaly at the AAD ridge crest is dynamically maintained. Thus the exact values of depth anomaly may not be well constrained for past times, but the map view of the depth anomaly may still be useful as a proxy for the past location of thinned oceanic crust. Calculation of the temporal variation of dynamic topography in this region is beyond the scope of this paper.

An important characteristic of the present-day depth anomaly centered on the discordance (Figure 1b) is that its trend (NNE on the Australian plate, SSE on the Antarctic plate) cuts across major fracture zones and is therefore oblique to the

spreading direction. This is significant because it means that the source of the depth anomaly must have migrated westward relative to the SEIR over time [*Marks et al.*, 1990]. Another feature is a pair of prominent depth anomaly lows, one located on the northern ridge flank at 128.5°E, 45°S, the other on the southern flank at 125.5°E, 54.5°S. These lows appear to have shared a common origin at the SEIR.

At Chron 6y time (Figure 4a) the depth anomaly is centered east of the discordance, and it trends roughly north-south near the spreading ridge, but including the large depth lows adjacent to the Australian and Antarctic margins suggests a more arcuate pattern. These large depth anomaly lows are poorly constrained because the sediments are thick and the seafloor ages are not derived from detailed surveys. By Chron 5ad time (14.4 Ma, Figure 4b), the characteristic arcuate shape of the depth anomaly is well defined; apparently, the source has started its westward migration relative to the SEIR and the fracture zones that cross it, and the depth anomaly is centered roughly on the ridge axis in corridor B5. A local depth anomaly low (<-800 m) is located in the center of the depth anomaly. Roughly 3.5 m.y. later, at Chron 5o time (Figure 4c), this local depth anomaly low has been split apart by seafloor spreading, and the regional depth anomaly has become more arcuate in shape as the source continued its apparent westward migration. By Chron 4 time (Figure 4d) the depth anomaly is centered on the ridge axis in corridor B4, and the conjugate depth anomaly lows are very evident on the northern and southern ridge flanks. The center of the depth anomaly continues to move westward relative to the transform faults along the spreading ridge through Chron 3y and Chron 2ay times (Figures 4e and 4f), and the prominent lows move farther away from the ridge due to seafloor spreading. By Chron 2ay time, the depth anomaly looks very much as it does presently (see Figure 1b) with the exception that a new local depth anomaly low is now centered between spreading corridors B3 and B4.

Our reconstructions show that at times older than ~14.4 Ma (Chron 5ad time) the regional depth anomaly trended more north-south and was centered east of the discordance zone. Since ~14.4 Ma, the locus of the depth anomaly has migrated westward relative to the SEIR at a rate of ~15 mm yr^{-1}, so that presently the depth anomaly is centered on the discordance. Our reconstructions also demonstrate that the two depth anomaly lows currently located on the northern and southern ridge flanks were juxtaposed at the spreading ridge axis at Chron 5ad time (14.4 Ma). If there is a direct relationship between the strength of the source and the magnitude of the depth anomaly, then we can infer that the source was stronger ~14 m.y. ago and then waned, and it has recently regained strength, as is evidenced by the local depth anomaly low presently located on the ridge axis.

Note that there are local asymmetries in the depth anomaly reconstructions; for example, at present, and thus also for some older times (e.g., Chron 2ay), the -400 m and -600 m depth anomaly contours are very close to one another on the Antarctic plate and much farther from one another on the Australia plate. If these depth anomalies strictly reflect the presence of thinner than normal oceanic crust, this would imply that the crustal thinning was not occurring symmetrically about the ridge axis. However, it is possible that some of this asymmetry is contributed by dynamic effects that we are not taking into account and which may not be centered on the modern ridge crest (see models by *Gurnis et al.* [1998]).

A comparison of the ridge crest geometry and the inferred depth anomaly through time suggests that the increased tectonic complexity of the discordance since 20 Ma appears to have occurred somewhat independently of the growth and westward migration of the regional depth anomaly. The changes in crenelation of the plate boundary geometry appear to be confined to the same AAD region of the ridge crest, showing a relatively steady increase in crenelation between Chrons 6y and 2ay. By contrast, the depth anomaly has migrated westward relative to the ridge crest and has not been increasing steadily in magnitude with time. At Chron 6y the depth anomaly underlies a zone of the ridge crest that has a relatively simple geometry, east of the zone of crenelated plate boundary geometry of the AAD. Thus, although the depth anomaly is now centered on the region of strong crenelation of the ridge crest, going back in time, the two types of changes are not very well correlated, neither spatially nor in terms of intensity.

It would be extremely useful to have detailed information on the magnetic anomaly pattern for older times, for example, the region of depth anomaly >1000 m and strong disruption of the gravity field, visible at the edges of the reconstructed region for Chron 6y (Figure 4a). Unfortunately, the sparse marine magnetic coverage of this part of the seafloor does not allow us to evaluate the degree to which the crenelation of the plate boundary might have varied in this region for times prior to Chron 6y. However, new detailed identifications of magnetic anomalies for Chrons 20 to 34y adjacent to the Australian and Antarctic margins (that include proprietary Japanese National Oil Corporation ship data) suggest that the paleo-Southeast Indian mid-ocean ridge was not crenelated [*Tikku and Cande*, 1999].

5. Implications for the Geodynamic Origin of the Discordance

A fundamental geochemical boundary between Pacific- and Indian-type mid-ocean ridge basalts (MORBs) has been identified in the discordance [e.g., *Klein et al.*, 1988]. This boundary presently lies in the eastern portion of spreading corridor B4, but it has moved westward (relative to the transform faults) with time; it only reached the eastern boundary of the discordance at Chron 2a [*Pyle et al.*, 1995]. Because of this geochemical boundary as well as the depth anomaly, the crenelated pattern of the plate boundary, variations in ridge morphology, and the propagation of ridge segments toward the discordance from both sides, it has been suggested that the discordance represents a boundary between two different mantle provinces, characterized by a magma deficit and thinner crust being produced along the mid-ocean ridge, possibly due to the presence of relatively cold mantle compared to adjacent spreading segments along the Australia-Antarctica boundary [e.g., *West et al.*, 1994, 1997].

Several models of the source of the discordance have been proposed to explain the observed characteristics. One model is of a "coldspot," which is a heat sink that is fixed in the mantle in which it is embedded [*Hayes*, 1976]; another model invokes convective flow with possible downwelling beneath the AAD [e.g., *Hayes*, 1988; *Klein et al.*, 1988]; others suggest that the AAD may be explained by passive along-axis flow in response to the cooler mantle temperatures beneath this part of the ridge axis [*Forsyth et al.*, 1987; *West et al.*, 1997]. The presence of inferred cooler mantle temperatures as well as the geochemical variation has recently been attributed to the presence

of material from a former subducted slab along the Gondwana margin, which is now being drawn up by convective upwelling into the AAD region of the SEIR [*Gurnis et al.*, 1998].

Each of these models predict distinctive depth anomaly patterns that can be compared with the observed arcuate-shaped depth anomaly (Figure 1b). *Marks et al.* [1990] performed this comparison and concluded that if the depth anomaly has a point source, it must migrate westward relative to the SEIR in order to produce the observed depth anomaly shape and symmetry about the spreading ridge axis. Thus a localized point source fixed in the mantle (e.g., a coldspot) was ruled out, as was a regular mantle convection pattern because absolute plate motions of the Australian and Antarctic plates would leave depth anomaly traces that do not match those observed. *Gurnis et al.* [1998] show that a line source fixed in the mantle, in this case a vestigial subducted slab, could match the map pattern of the observed depth anomaly.

Although both the depth anomaly and the crenelation pattern are considered to be fundamental characteristics of the AAD, the research presented here is the first to recognize that the crenelation pattern has not migrated westward with the depth anomaly. A successful model for the source of the AAD must account for our findings that the center of the crenelated zone has not migrated westward along the SEIR as has the locus of the depth anomaly, that the crenelation of the plate boundary has increased with time, and that the fundamental isotopic boundary has migrated westward but at a faster rate (25 mm yr^{-1} since 4 Ma [*Pyle et al.*, 1995]) than the depth anomaly (15 mm yr^{-1} since 15 Ma [*Marks et al.*, 1990]).

We find it difficult to attribute the unstable history of the B3-B4 boundary, or other unstable boundaries within the AAD, to the close proximity of the geochemical boundary because the position of the geochemical boundary has moved westward with time. It is interpreted that Pacific-type upper mantle flowed toward the discordance from the east, thus migrating westward to its present position even though the B3-B4 boundary displayed unstable behavior since its inception nearly 20 m.y. ago. However, a recent detailed analysis of dense ship data collected in corridor B4 near the ridge axis demonstrates that the B4 spreading ridge is starved for magma and that separation between Australian and Antarctic seafloor at least in this spreading corridor has been dominated in recent times by amagmatic extension (e.g., listric faulting) [*Christie et al.*, 1998]. An uneven supply of magma to adjacent ridge segments could possibly contribute to their lengthening or shortening, with the common boundary adjusting to the changes in length accordingly. We suggest that a temporal variation (such as an increase in the amount of cooler mantle upwelling within the AAD) has led to the production of thin crust and/or episodes of amagmatic extension and the subsequent growth of the crenelated ridge pattern within the AAD since Chron 6y time.

This crenelation may arise as a consequence of the extreme degree of amagmatic extension. It has been suggested that in the case of hotspots, relief on the base of the lithosphere can function as an upside-down drainage pattern that traps plume material and funnels it toward regions where the base of the lithosphere is shallowest [*Sleep*, 1996, 1997]. Perhaps the same effect may also localize the asthenospheric partial melts forming the mid-ocean ridge system. Normally, we envision that the lithosphere is thinnest at the ridge crest and that melts will be naturally focused up into the axial region, resulting in symmetric spreading. However, if there is enough of a magma deficit so that a high percentage of the plate motion is accomplished by amagmatic extension [*Christie et al.*, 1998], a more complicated geometry of the base of the lithospheric plate may result. For example, active extensional faults away from the ridge crest might produce local shallowing of the base of the lithosphere tens of kilometers away from the active ridge. In this case, perhaps the asthenospheric melts being produced would be able to focus in these local highs, eventually leading to a "ridge jump" wherein seafloor spreading ceases at the original ridge axis and takes hold in the new location. Such processes could produce an overall pattern of asymmetric spreading which varies from segment to segment along the plate boundary, according to the local geometry and map pattern of the extensional faults. In such a case, local tectonics would essentially control the evolution of the crenelation pattern if enough of a magma deficit persisted over time.

The major implication of our study is that the development of the discordance is an ongoing process; the length of the plate boundary within the discordance has been progressively increasing over time. This lengthening is not perfectly correlated with the development and migration of the depth anomaly. Although steady state models of mantle flow may be adequate to explain the lateral migration of isotopic boundaries and/or of the depth anomaly, they probably cannot explain the temporal variations seen in the ridge crest geometry. Models involving no temporal changes in mantle temperature or in along-axis flow patterns over time would not necessarily be expected to produce a continuous increase in crenelation of the plate boundary. If, however, mantle temperature in this region were changing with time (e.g., if material from a cold slab at depth is being drawn up beneath the AAD [e.g., *Gurnis et al.*, 1998]), temporal variations in the amount and position of this material might be expected and could plausibly cause temporal and spatial changes in the depth anomaly and in the crenelation of the plate boundary. The lack of a detailed correlation between the depth anomaly and the plate boundary crenelation suggests that the processes responsible for plate boundary crenelation may be more local effects (e.g., local magma deficit along certain segments of the ridge axis; excessive tectonic extension and/or small ridge jumps moving the locus of spreading in individual spreading segments), whereas the depth anomaly, at least filtered at the level we are examining it, has a broader, regional control.

6. Summary

We have reconstructed gravity and depth anomalies covering the Australian-Antarctic discordance, at selected ages younger than 20 Ma. Satellite-derived marine gravity anomalies are ideal for determining the tectonic development of a complex region such as the AAD because fracture zones, transform faults, ridge axes, and other fine-scale details of the seafloor are accurately mapped and located. The depth anomalies, on the other hand, have been effectively band-pass filtered because a depth-age relation has been removed from the bathymetric depths, and anomalies with wavelengths shorter than 400 km have been eliminated. The resulting depth anomalies thus do not map details but rather reflect broader, more regional departures of the bathymetric depths from what would be expected based on normal lithospheric cooling models.

Our reconstructions that depict the gravity and depth anomalies as they would appear in the past reveal the following: (1) prior to 19 Ma, the discordance segment of the SEIR consisted

of three large fracture zones and a large eastward pointing propagating rift wake, (2) since 19 Ma, numerous other fracture zones and pseudofaults have formed in the discordance, some of which changed from pseudofaults to fracture zones or vice versa, (3) some pseudofaults have switched propagation direction, (4) the major fracture zones that bound spreading corridor B5 and that bound the discordance on the east and west have persisted since before 19 Ma, (5) the length of the plate boundary within the discordance has been increasing since 19 Ma, (6) the depth anomaly has migrated westward at a rate of ~15 mm yr^{-1} since at least Chron 5ad time, (7) the zone of crenelation of the plate boundary in the discordance is either stationary or migrating much more slowly relative to the ridge axis, and (8) the strength of the depth anomaly has waxed and waned over time, with increases in strength occurring at about 14.4 Ma and again at the present time.

We find that the boundary changes from pseudofaults to fracture zones and vice versa cannot be explained by changes in the finite rotation pole. The B3-B4 boundary, which has been, at different times, either a fracture zone, pseudofault, or transform fault, may be a tectonic response to an uneven supply of magma to adjacent ridge segments. The 15 mm yr^{-1} westward migration of the depth anomaly to its current location is slower than the 25 mm yr^{-1} (since 4 Ma) rate of western migration of the isotopic boundary [*Pyle et al.*, 1995], so there is not a clear relationship between the depth anomaly and the flow of Pacific-type upper mantle from the east. There also does not appear to be a tie between the locus of the depth anomaly and the geometric complexity of the discordance. The westward migration of the depth anomaly from east of the discordance to its present location in the center of the AAD appears independent of the increasing number of fracture zones and propagating rifts within and to the west of the AAD. Thus we think the source of the depth anomaly is seated deeper in the mantle, while the tectonic complexities and increasing crenelation of the plate boundary through time are produced by either an uneven supply of magma to the ridge segments within and adjacent to the AAD, local variations in tectonic extension and ridge jumps along individual spreading segments, or the combination of thin crust with somewhat cooler upper mantle that other researchers have proposed.

Acknowledgments. Reviews from Dietmar Mueller, Donna Jurdy, and an anonymous referee improved this manuscript. We thank J. Zachariasen for working on the finite rotation parameters for Chron 6y, and Amotz Agnon and Mike Gurnis for helpful discussions. This project was partially supported by NSF grant EAR-9296102 to J. M. Stock. K. Quinn's participation was supported by the Summer Undergraduate Research Fellowship (SURF) program of the California Institute of Technology. Contribution 8535, California Institute of Technology, Division of Geological and Planetary Sciences. The magnetic anomaly identifications, finite rotation parameters, and images of the reconstructions are available on the Worldwide Web site http://ibis.grdl.noaa.gov/SAT/kmm/aad.intro.html.

References

Abelson, M., and A. Agnon, Mechanics of oblique spreading and ridge segmentation, *Earth Planet. Sci. Lett.*, *148*, 405–421, 1997.

Cande, S. C., and D. V. Kent, Revised calibration of the geomagnetic polarity time scale for the Late Cretaceous and Cenozoic, *J. Geophys. Res.*, *100*, 6093–6096, 1995.

Cande, S. C., and J. C. Mutter, A revised identification of the oldest sea-floor spreading anomalies between Australia and Antarctica, *Earth Planet. Sci. Lett.*, *58*, 151–160, 1982.

Chang, T., On the statistical properties of estimated rotations, *J. Geophys. Res.*, *92*, 6319–6329, 1987.

Chang, T., Estimating the relative rotation of two plates from boundary crossings, *JASA*, *J. Am. Stat. Assoc.*, *83*, 1178–1183, 1988.

Christie, D. M., B. P. West, D. G. Pyle, and B. B. Hanan, Chaotic topography, mantle flow, and mantle migration in the Australian-Antarctic discordance, *Nature*, *394*, 637–644, 1998.

Cochran, J. R., Variations in subsidence rates along intermediate and fast spreading mid-ocean ridges, *Geophys. J. R. Astron. Soc.*, *87*, 421–454, 1986.

Forsyth, D. W., R. L. Ehrenbard, and S. Chapin, Anomalous upper mantle beneath the Australian-Antarctic discordance, *Earth Planet. Sci. Lett.*, *84*, 471–478, 1987.

Gurnis, M., R. D. Muller, and L. Moresi, Cretaceous vertical motion of Australia and the Australian-Antarctic discordance, *Science*, *279*, 1499–1504, 1998.

Hayes, D. E., Nature and implications of asymmetric sea-floor spreading—Different rates for different plates, *Geol. Soc. Am. Bull.*, *87*, 994–1002, 1976.

Hayes, D. E., Age-depth relationships and depth anomalies in the southeast Indian Ocean and South Atlantic Ocean, *J. Geophys. Res.*, *93*, 2937–2954, 1988.

Hellinger, S. J., The uncertainties of finite rotations in plate tectonics, *J. Geophys. Res.*, *86*, 9312–9318, 1981.

Klein, E. M., C. H. Langmuir, A. Zindler, H. Staudigel, and B. Hamelin, Isotope evidence of a mantle convection boundary at the Australian-Antarctic discordance, *Nature*, *333*, 623–629, 1988.

Lonsdale, P., Segmentation and disruption of the East Pacific Rise in the mouth of the Gulf of California, *Mar. Geophys. Res.*, *17*, 323–359, 1995.

Marks, K. M., and J. M. Stock, High-precision location of fracture zones in Geosat data: The Macquarie triple junction region, *Eos Trans. AGU*, *72*(44), Fall Meet. Suppl., F444, 1991.

Marks, K. M., and J. M. Stock, Asymmetric seafloor spreading and short ridge jumps in the Australian-Antarctic discordance, *Mar. Geophys. Res.*, *17*, 361–373, 1995.

Marks, K. M., and J. M. Stock, Early Tertiary gravity field reconstructions of the southwest Pacific, *Earth Planet. Sci. Lett.*, *152*, 267–274, 1997.

Marks, K. M., P. R. Vogt, and S. A. Hall, Residual depth anomalies and the origin of the Australian-Antarctic discordance zone, *J. Geophys. Res.*, *95*, 17,325–17,337, 1990.

Marks, K. M., D. C. McAdoo, and W. H. F. Smith, Mapping the Southwest Indian Ridge with Geosat, *Eos Trans. AGU*, *74*(8), 81–86, 1993.

McAdoo, D. C., and K. M. Marks, Gravity fields of the Southern Ocean from Geosat data, *J. Geophys. Res.*, *97*, 3247–3260, 1992.

Menard, H. W., Depth anomalies and the bobbing motion of drifting islands, *J. Geophys. Res.*, *78*, 5128–5137, 1973.

Morgan, G. A., H. S. Fleming, and R. H. Feden, Project Investigator 1: A cooperative US/Australian airborne geomagnetic study south of Australia, paper presented at 13th International Symposium on Remote Sensing of the Environment, Environ. Res. Inst. of Mich., Ann Arbor, Mich., 1979.

Müller, R. D., W. R. Roest, J.-Y. Royer, L. M. Gahagan, and J. G. Sclater, Digital isochrons of the world's ocean floor, *J. Geophys. Res.*, *102*, 3211–3214, 1997.

National Geophysical Data Center, Digital relief of the surface of the Earth, Data Announce. 88-MGG-02, U.S. Dep. of Commer., Natl. Oceanic and Atmos. Admin., Boulder, Colo., 1988.

National Geophysical Data Center, Worldwide marine geophysical data, version 3.3 [Geodas CD-ROM], Data Announce. 97-MGG-01, U.S. Dep. of Commer., Natl. Oceanic and Atmos. Admin., Boulder, Colo., 1997.

Pyle, D. G., D. M. Christie, J. J. Mahoney, and R. A. Duncan, Geochemistry and geochronology of ancient southeast Indian and southwest Pacific seafloor, *J. Geophys. Res.*, *100*, 22,261–22,282, 1995.

Royer, J.-Y., and T. Chang, Evidence for relative motions between the Indian and Australian plates during the last 20 m.y. from plate tectonic reconstructions: Implications for the deformation of the Indo-Australian plate, *J. Geophys. Res.*, *96*, 11,779–11,802, 1991.

Royer, J.-Y., and R. G. Gordon, The motion and boundary between the Capricorn and Australian plates, *Science*, *277*, 1268–1274, 1997.

Sandwell, D. T., and W. H. F. Smith, Marine gravity anomaly from Geosat and ERS 1 satellite altimetry, *J. Geophys. Res.*, *102*, 10,039–10,054, 1997.

Sleep, N. H., Lateral flow of hot plume material ponded at sublithospheric depths, *J. Geophys. Res.*, *101*, 28,065–28,083, 1996.

Sleep, N. H., Lateral flow and ponding of starting plume material, *J. Geophys. Res.*, *102*, 10,001–10,012, 1997.

Smith, W. H. F., and D. Sandwell, Bathymetric prediction from dense satellite altimetry and sparse shipboard bathymetry, *J. Geophys. Res.*, *99*, 21,803–21,824, 1994.

Tikku, A. A., and S. C. Cande, The oldest magnetic anomalies in the Australian-Antarctic basin: Are they isochrons?, *J. Geophys. Res.*, in press, 1999.

Tolstoy, M., A. J. Harding, J. A. Orcutt, and J. Phipps Morgan, Crustal thickness at the Australian-Antarctic discordance and neighboring Southeast Indian Ridge, *Eos Trans. AGU*, Fall Meet. Suppl., *76*(46), F570, 1995.

Tucholke, B., and H. Schouten, The Kane Fracture Zone, *Mar. Geophys. Res.*, *10*, 1–39, 1989.

Turcotte, D. L., and E. R. Oxburgh, Convection in a mantle with variable physical properties, *J. Geophys. Res.*, *74*, 1458–1474, 1969.

Vogt, P. R., N. Z. Cherkis, and G. A. Morgan, Project Investigator-1: Evolution of the Australia-Antarctic discordance deduced from a detailed aeromagnetic study, in *Antarctic Earth Science*, edited by R. L. Oliver, P. R. James, and J. B. Jago, pp. 608–613, Aust. Acad. of Sci., Canberra, 1983.

Weissel, J. K., and D. E. Hayes, The Australian-Antarctic discordance: New results and implications, *J. Geophys. Res.*, *79*, 2579–2587, 1974.

West, B. P., J.-C. Sempere, D. G. Pyle, J. Phipps Morgan, and D. M. Christie, Evidence for variable upper mantle temperature and crustal thickness in and near the Australian-Antarctic discordance, *Earth Planet. Sci. Lett.*, *128*, 135–153, 1994.

West, B. P., W. S. D. Wilcock, and J.-C. Sempere, Three-dimensional structure of asthenospheric flow beneath the Southeast Indian Ridge, *J. Geophys. Res.*, *102*, 7783–7802, 1997.

K. M. Marks, Laboratory for Satellite Altimetry, National Oceanic Data Center, NOAA, E/OC2,1315 East-West Highway, SSMC 3, sta. 3855, Silver Spring, MD 20910-3282. (kmarks@nodc.noaa.gov)

K. J. Quinn, Department of Earth and Planetary Sciences, Massachusetts Institute of Technology, 77 Massachusetts Avenue, Room 54-616, Cambridge, MA 02139. (katyq@mit.edu)

J. M. Stock, Seismological Laboratory, California Institute of Technology, Caltech 252-21, Pasadena, CA 91125. (jstock@gps.caltech.edu)

(Received April 22, 1998; revised October 13, 1998;
accepted October 21, 1998.)